

MAD accretion disks and structured jets for GRB and AGN

Agnieszka Janiuk
Center for Theoretical Physics PAS

CPB meeting
Brno, 03.06.2022

Agnieszka Janiuk, CFT PAN



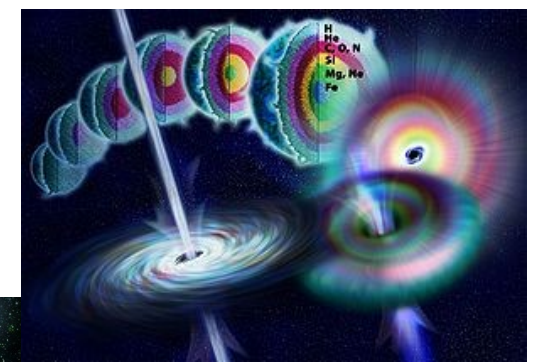
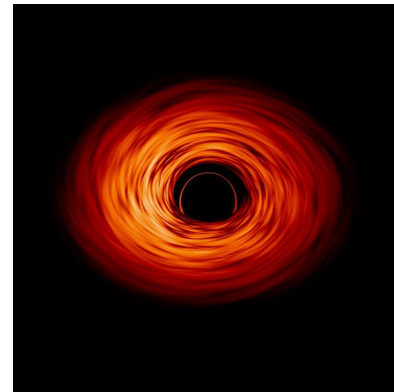
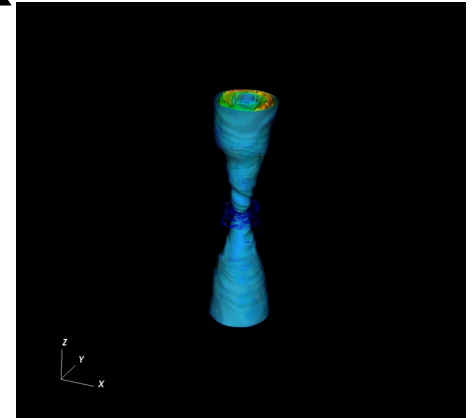
Content of the talk

1. Introduction, GRBs and AGN.

2. Black hole – jet accretion disk central engine, numerical simulations

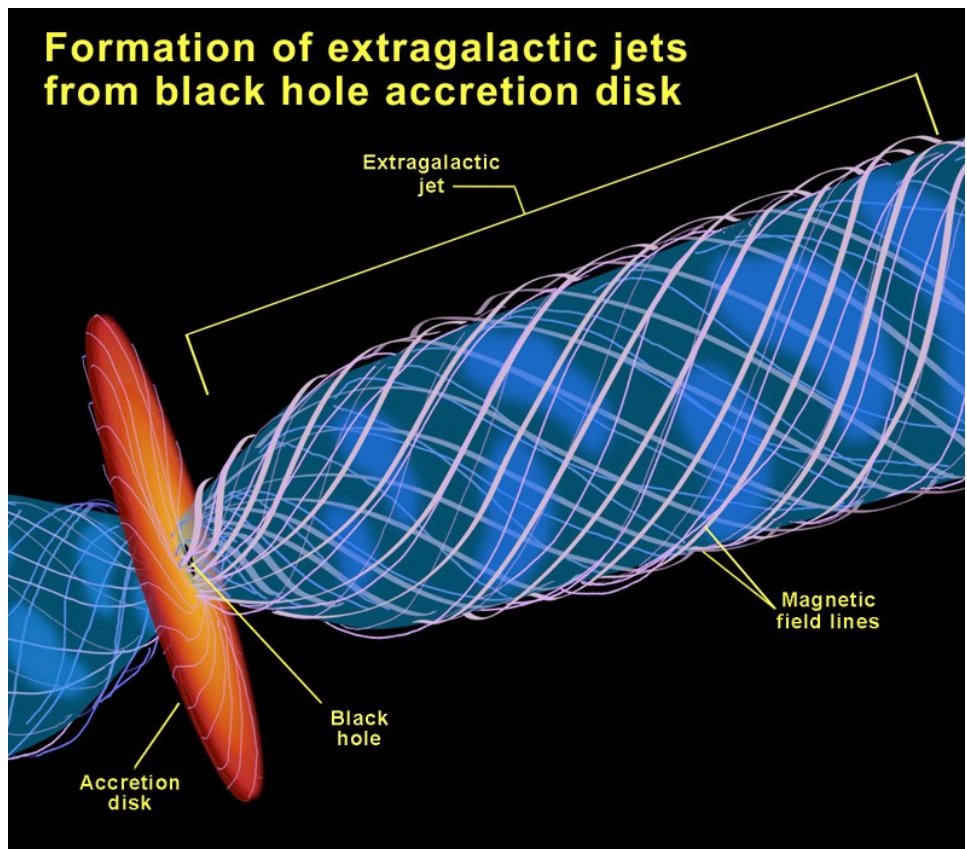
3. Jet-wind interaction in short GRBs and kilonova emission

4. Polarisation of the emission from BH horizon vicinity



Relativistic jets paradigm

Jets are common in the Universe
Observed at different mass scales
from accreting black holes
Need a central engine
Magnetic fields anchored in the
accretion disk penetrate black
hole's ergosphere and mediate
extraction of its rotational energy
Spinning black hole twists open
field lines, helping the jet
collimation



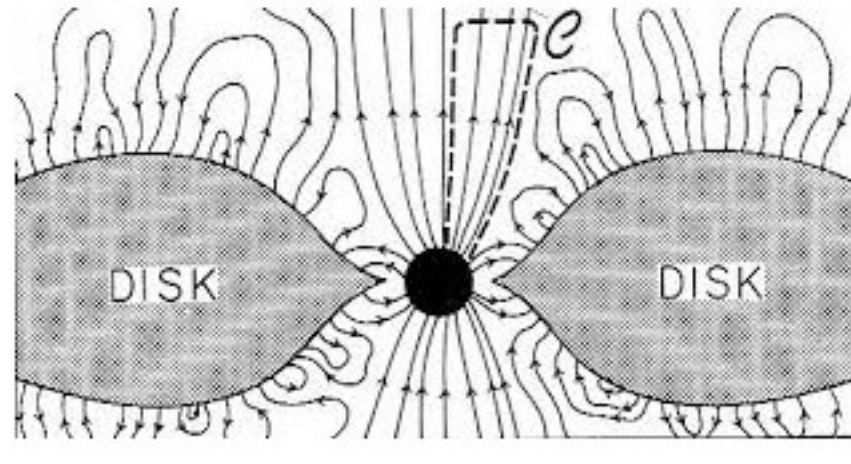
Powering of jets

Extracted power

$$\dot{E}_{\text{BZ}} = \frac{\kappa}{4\pi} \Phi_{\text{BH}}^2 \frac{a^2 c}{16r_g^2}$$

$$\Phi_{\text{BH}} = \frac{1}{2} \int |B^r| dA_{\theta\phi}$$

$$a = \frac{c J_{\text{BH}}}{G M_{\text{BH}}^2}$$



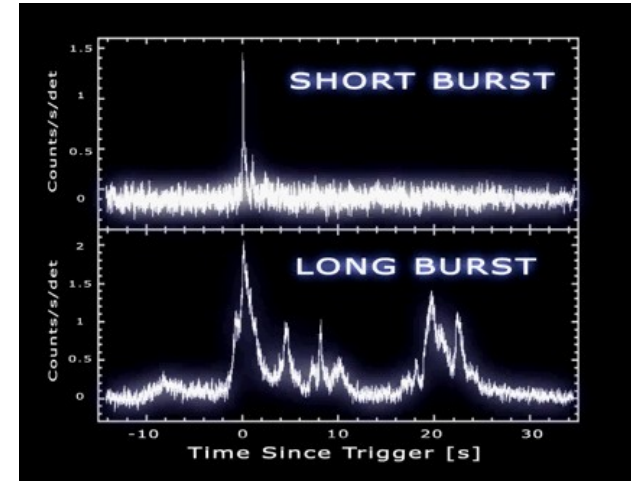
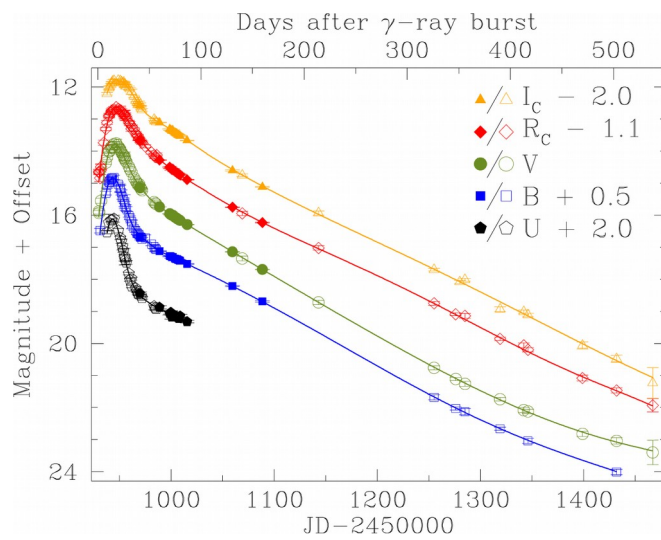
By analogy to pulsar magnetosphere, the field lines accelerate charged particles (Godreich & Julian 1969; Blandford & Znajek 1977)

Black hole magnetosphere develops from seed magnetic field by differential rotation of the disk (Thorne 1986)

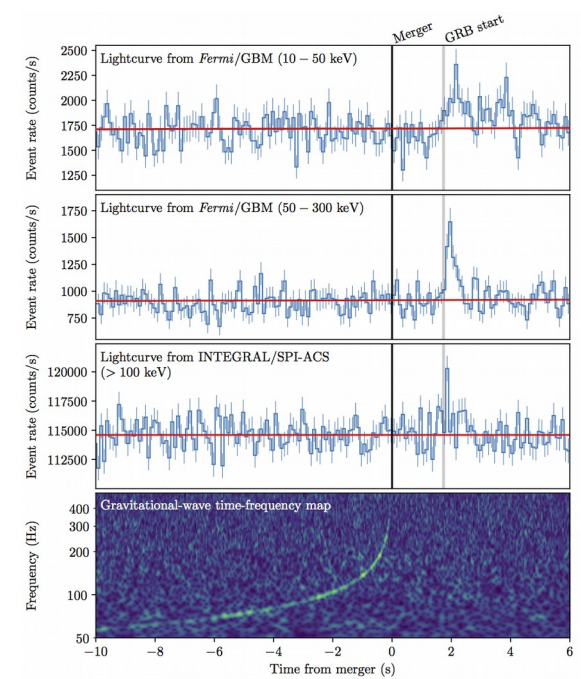
Gamma Ray bursts

Rapid, bright flashes of radiation peaking in the gamma-ray band

First association of long event:
GRB 980425 and SN 1998bw
(Kuulkarni et al. 1998)

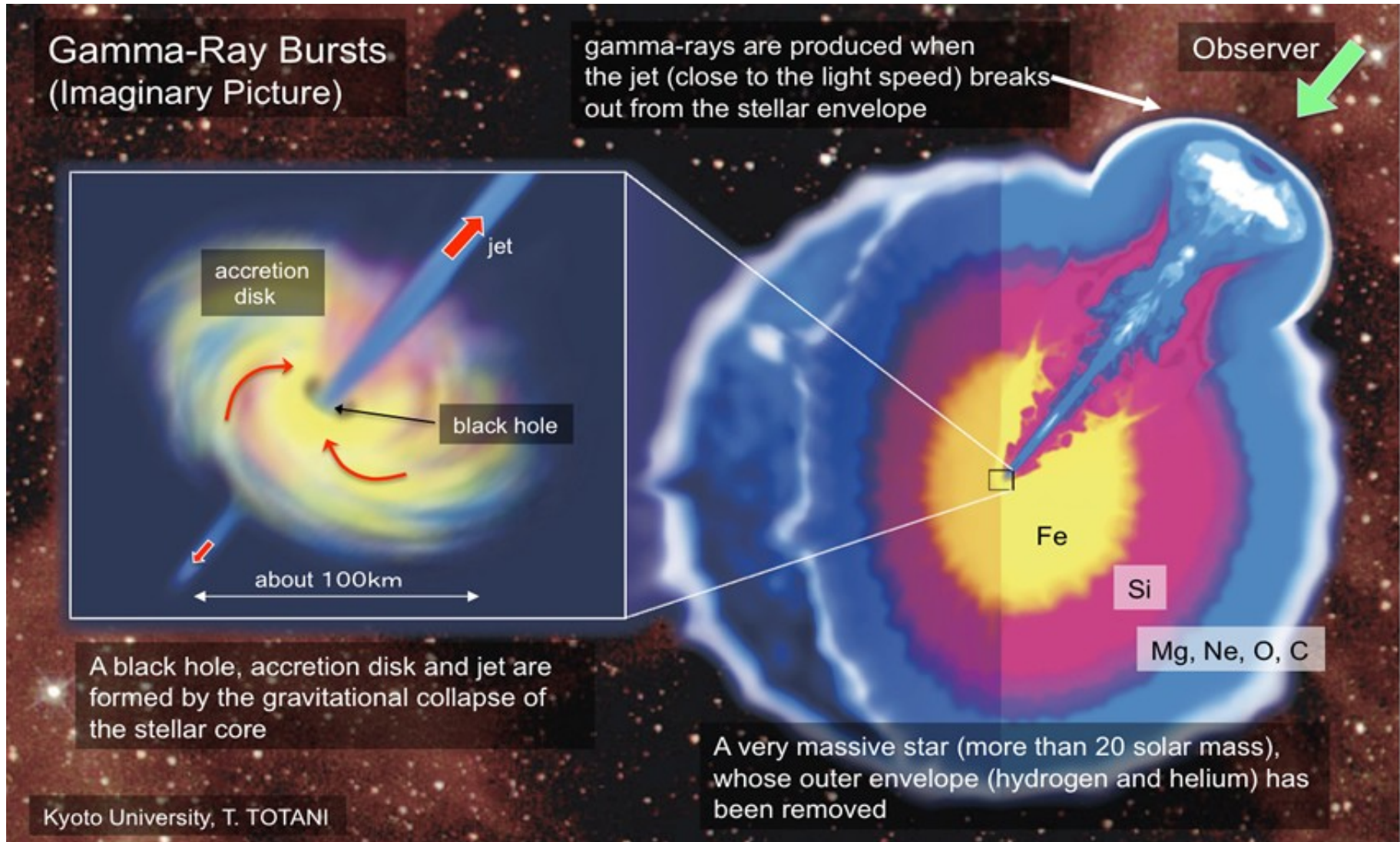


Confirmed source of short GRB:
GW170817
(Abbott et al. 2017)

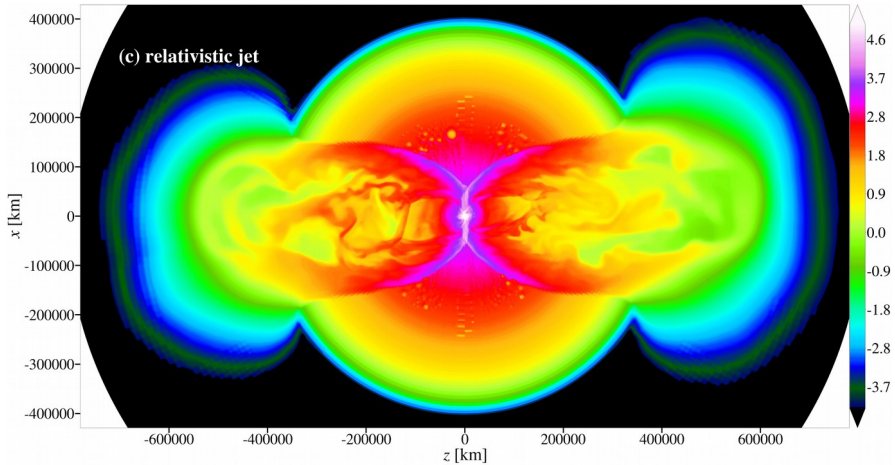


Complete lightcurve from Clochiatti et al. (2011)

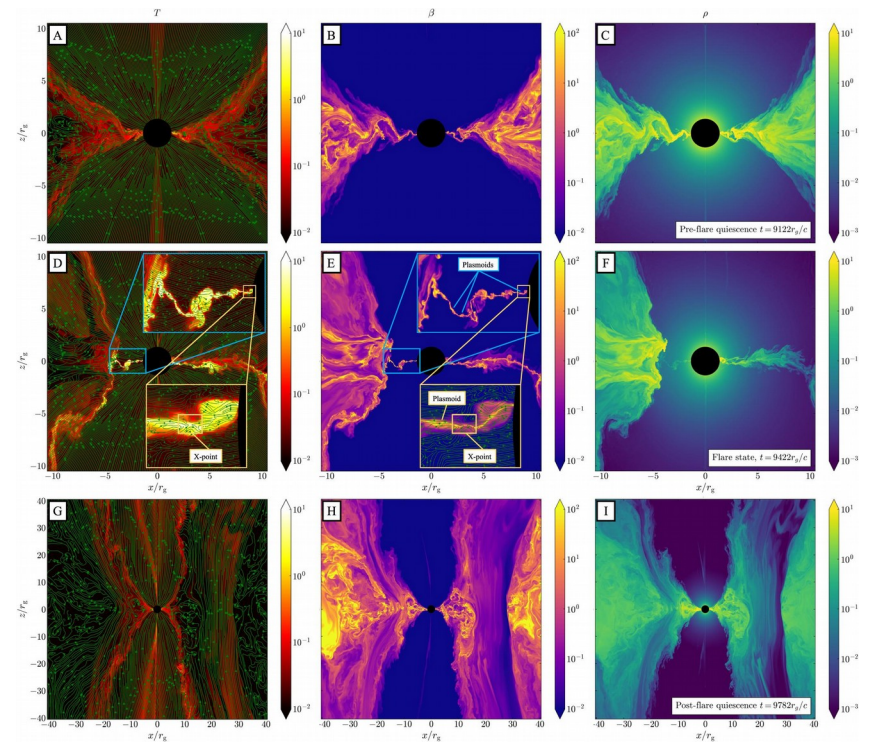
Long GRBs: collapsing massive stars



Collapsar simulation challenges

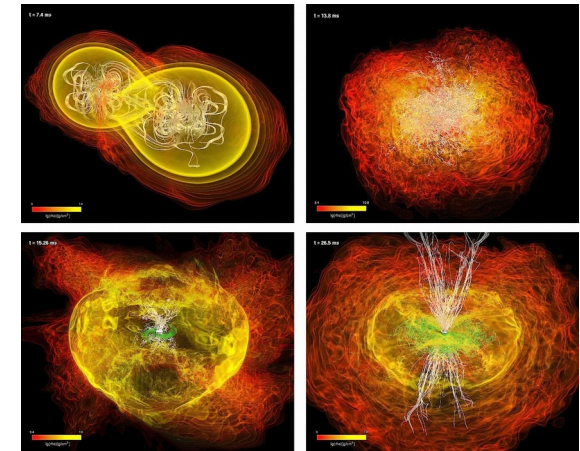
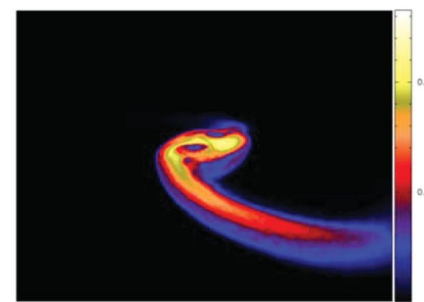
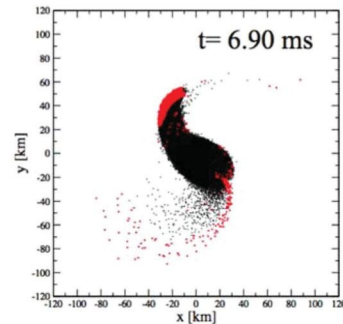
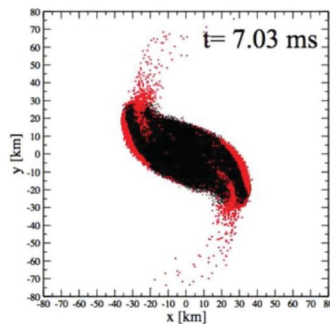


Jet breakout process difficult to model due to multi-scale problem and computational complexity (Gottlieb et al. 2022).

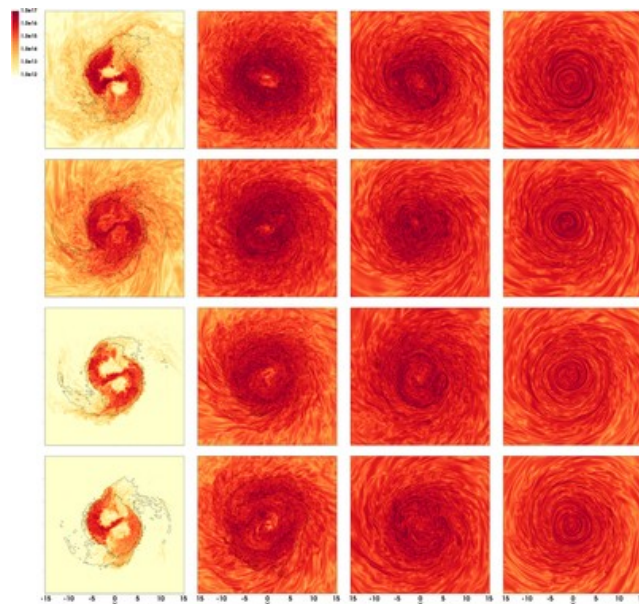


Very high resolution 3D simulations show also importance of plasmoid reconnection (Ripperda et al. 2022)

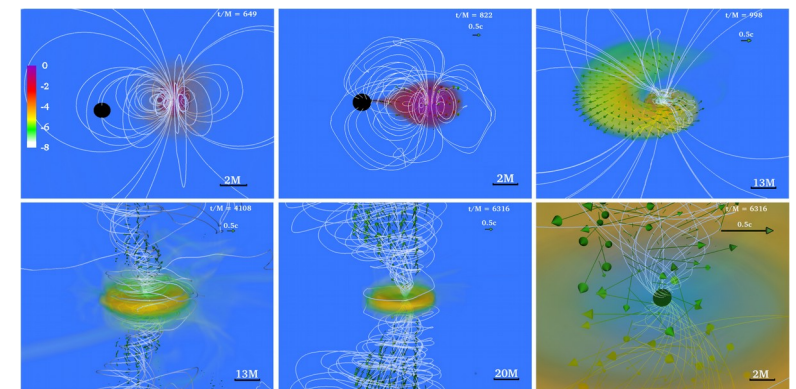
Short GRBs: Compact binary mergers



Korobkin *et al.* 2012



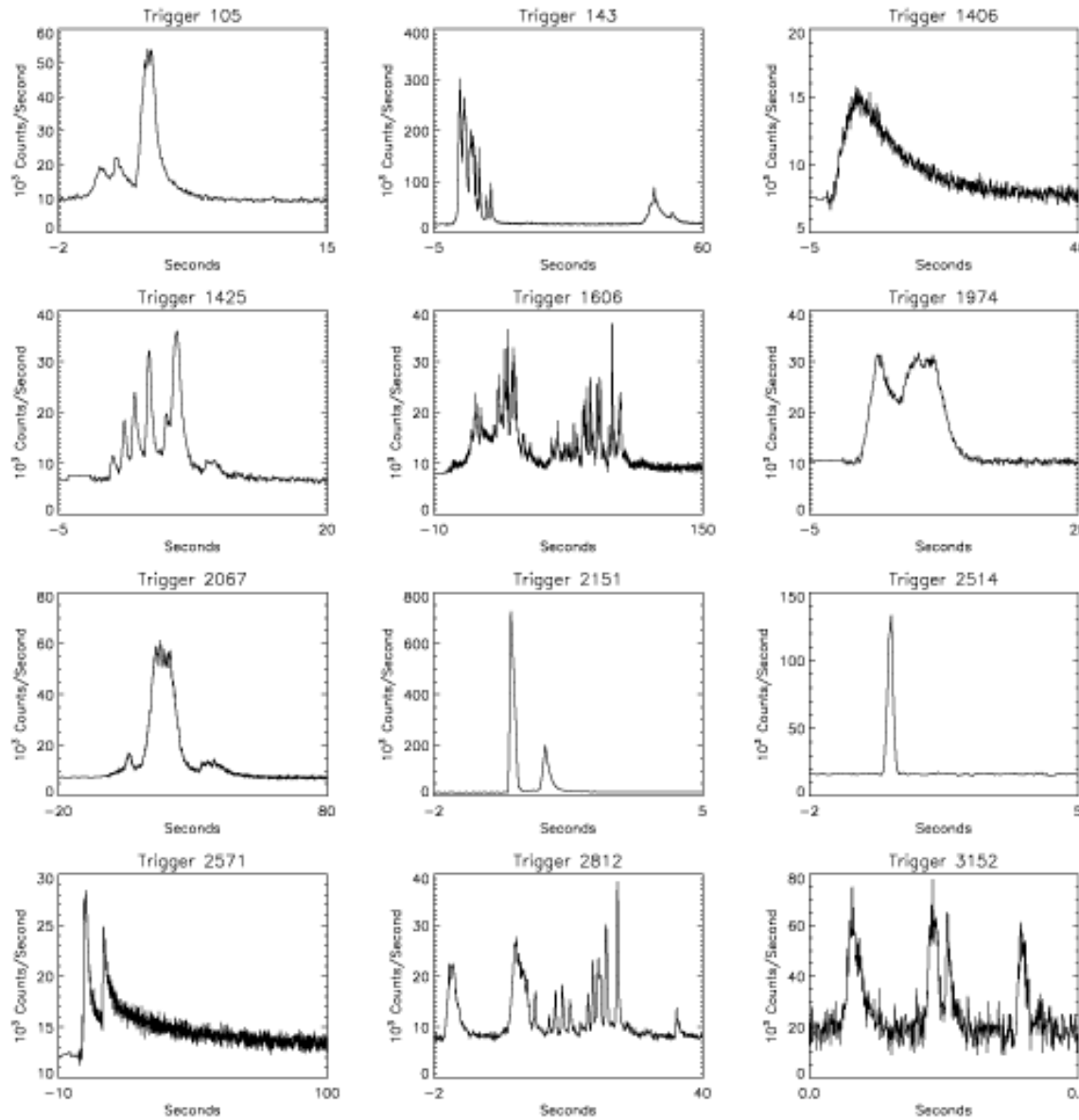
Rezzolla *et al.* 2014



Paschalidis *et al.* 2015

Aguilera-Miret, Vigano & Palenzuela, 2021

GRB variability

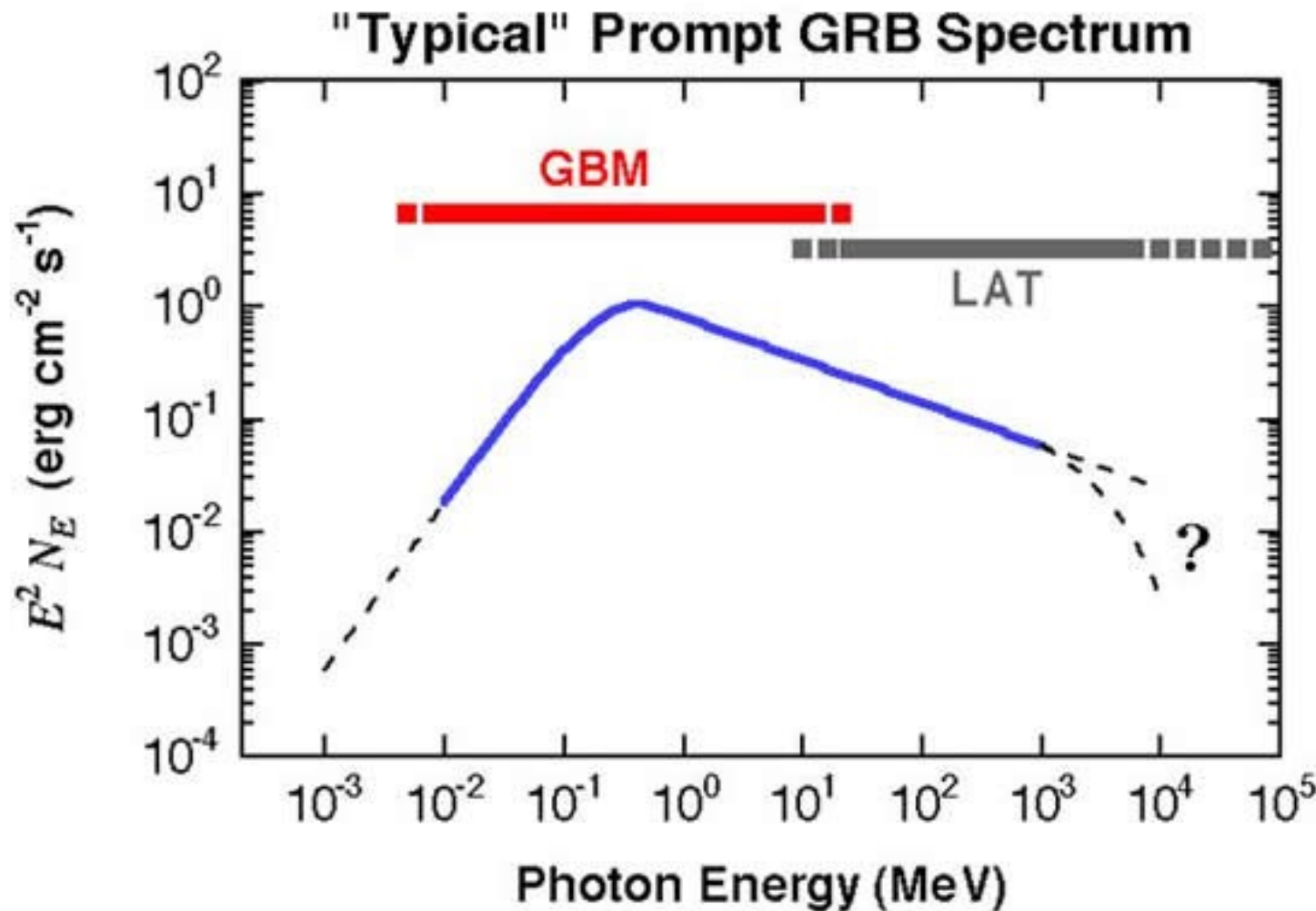


No two gamma-ray bursts are the same, as can be seen from this sample of a dozen light curves.

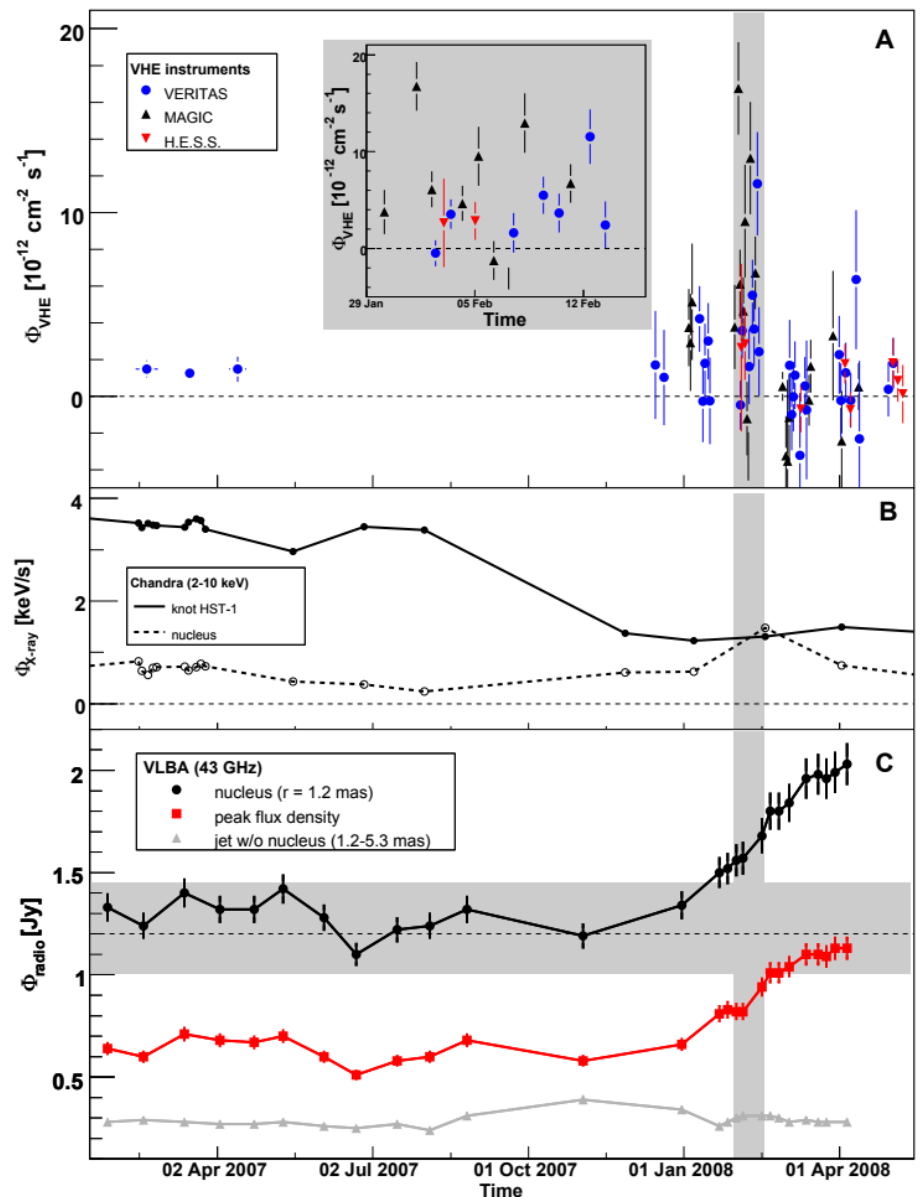
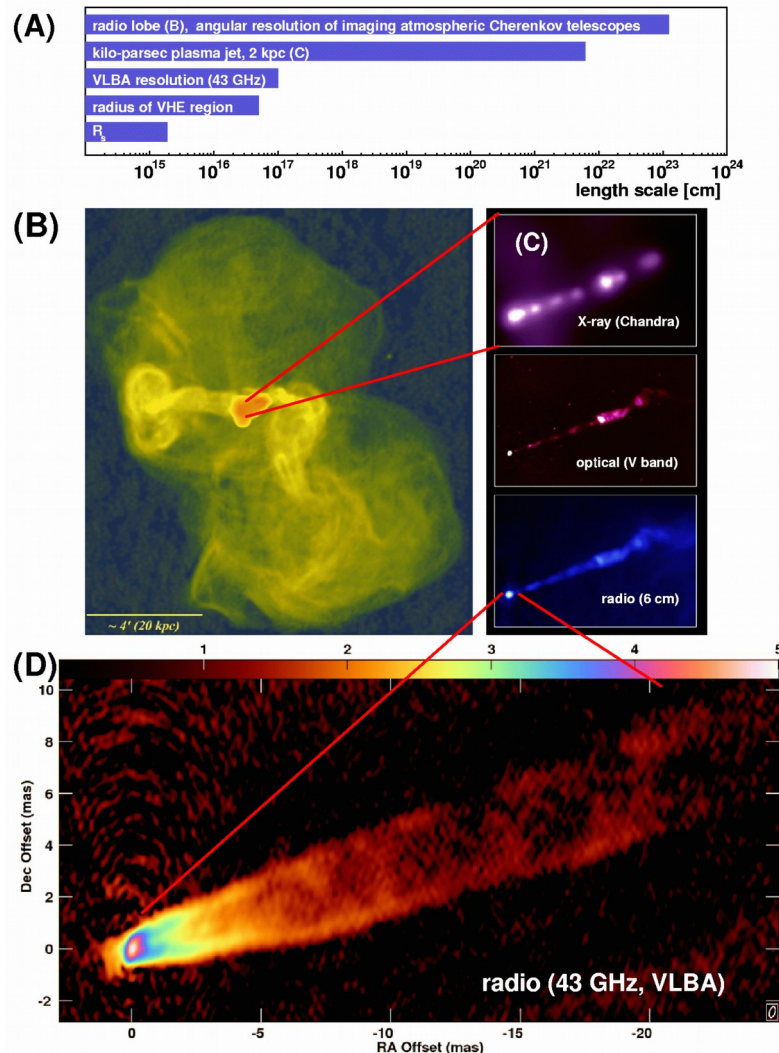
Some are short, some are long, some are weak, some are strong, some have more spikes, some have none, each unlike the other one.

Credit: NASA

Spectra of GRBs



AGN

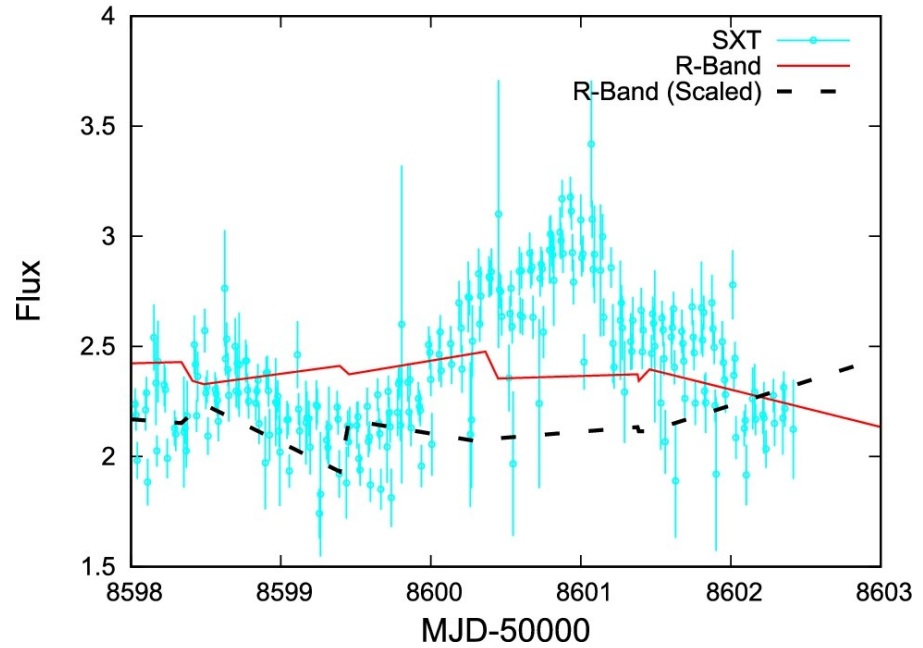


Multiwavelength images and variability of M87
in very high energies (Acciari et al. 2009)

Blazars

Type of active galaxies where non-thermal radiation produced in relativistic jet points into our line of sight

X-ray lightcurves show rapid variability of count rate, down into intra-day (minute) time scales and up to 4 magnitude amplitudes



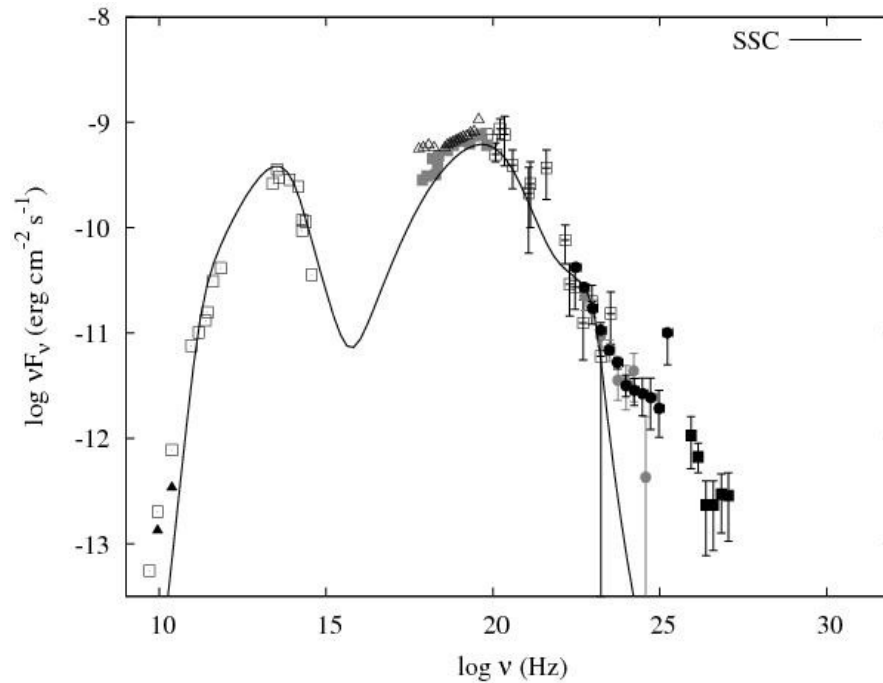
Mrk 501 observed by Astrosat
(Apil 2019); Chatterjee et al.
2021

Blazar emission spectra

SSC is an Inverse-Compton radiation produced when synchrotron radiation is upscattered by their own emitting particles

The one-zone SSC model is popular emission model due to simplicity and small number of free parameters (Mastichiadis & Kirk 1997; Ghisellini et al. 1998)

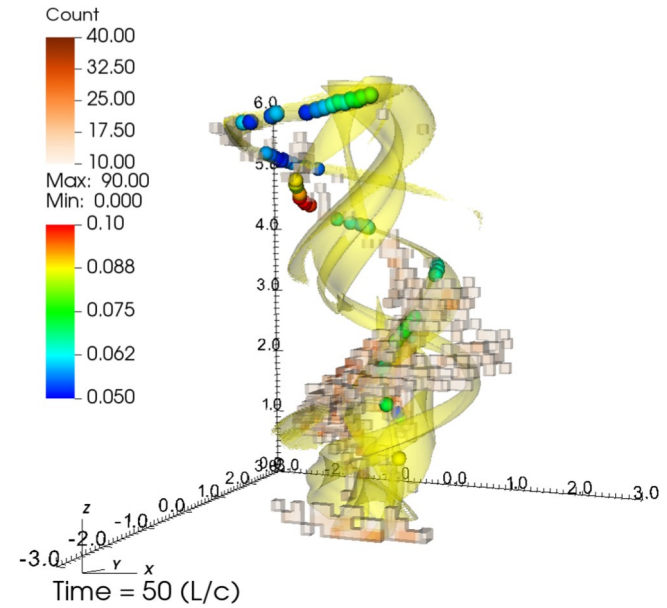
Some features of high energy spectra, at few GeV, are not explained by this model, and photo-hadronic interactions are proposed



Spectrum of Centaurus-A, and
SSC model fit;
(Petropoulou et al., 2014)

Blazar variability

Variability time-scales seen in PKS 2155-304 and Mrk 501 are much shorter than inferred light-crossing times at the black hole horizon, suggesting that the variability involves enhanced emission in a small region within an outflowing jet.

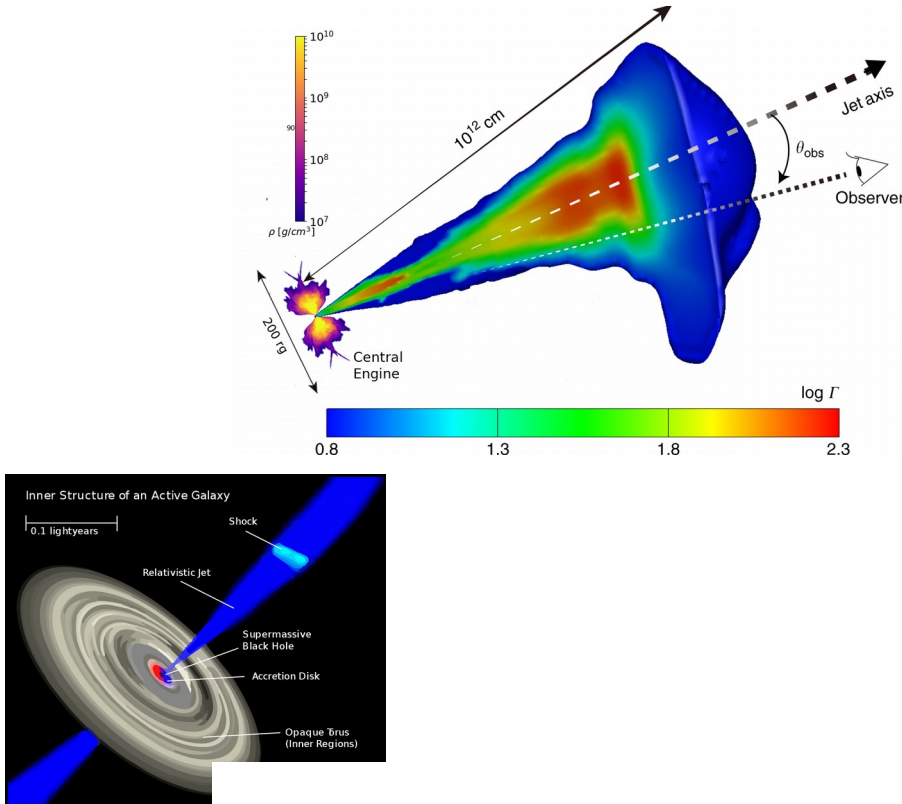


Lorentz factors must be at least $\Gamma \sim 50$, to prevent re-absorption of gamma rays by electron-positron pair creation (Begelman et al. 2008)

Particle acceleration occurs at sub-pc scales in magnetic reconnection sites

Accelerated particles interact with ambient photons and produce pions, then decay to γ 's and ν 's (Medina-Torrejon et al. 2021)

GRB and AGN Central engine



Gamma ray emission comes from the photosphere of a collimated relativistic outflow pushing through the interstellar medium.

Jet launching mechanism similar in GRB and AGN jets, across the mass scale.

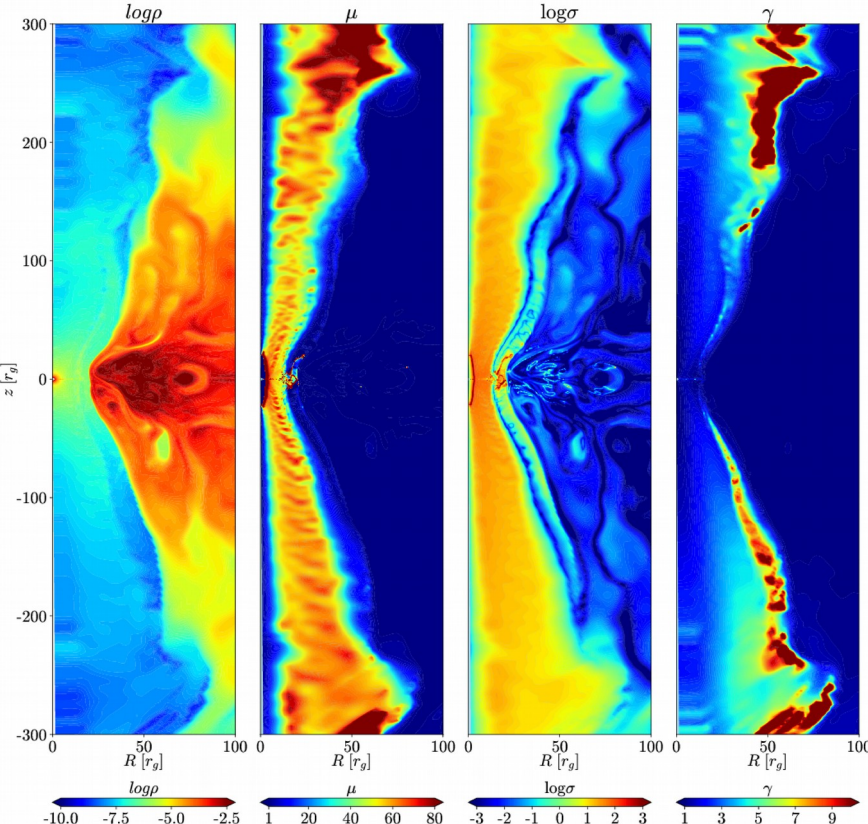
Quantitative differences:

- mass and density of disk
- magnetic flux
- Lorentz factors
- power of jet

Source	M_{BH} (M_\odot)	M_{disk}^{unit} (M_\odot)	Time ^{unit}	\dot{M}^{unit}	\dot{E}^{unit} (erg s ⁻¹)	D^{unit} (g cm ⁻³)	B ^{unit} (G)	Φ_B^{unit}
Short GRB	3	$1.5 \cdot 10^{-5}$	1.5×10^{-5} s	$1 M_\odot s^{-1}$	$1.8 \cdot 10^{54}$	$3.4 \cdot 10^{11}$	$6.2 \cdot 10^{16}$	$1.2 \cdot 10^{28}$ G cm ²
Long GRB	10	$1.5 \cdot 10^{-4}$	4.9×10^{-5} s	$3 M_\odot s^{-1}$	$5.5 \cdot 10^{54}$	$9.5 \cdot 10^{10}$	$3.2 \cdot 10^{16}$	$7.0 \cdot 10^{28}$ G cm ²
Sgr A*	$4 \cdot 10^6$	$6.2 \cdot 10^{-10}$	6.2×10^{-7} yr	$10^{-3} M_\odot \text{yr}^{-1}$	$5.6 \cdot 10^{43}$	$6.0 \cdot 10^{-12}$	$2.6 \cdot 10^5$	$9.0 \cdot 10^{-8}$ G pc ²
M 87	$5 \cdot 10^9$	$7.8 \cdot 10^{-7}$	7.8×10^{-4} yr	$10^{-3} M_\odot \text{yr}^{-1}$	$5.6 \cdot 10^{43}$	$3.8 \cdot 10^{-18}$	$2.6 \cdot 10^2$	$1.2 \cdot 10^{-5}$ G pc ²

Table 3. Conversion units for various astrophysical sources

Jet launching and energetics



$$\mu = \frac{-T_t^r}{\rho u^r} \quad \sigma = \frac{(T_{EM})_r^t}{(T_t^r)_{gas}}$$

$$\mu = \gamma h (1 + \sigma)$$

- The presence of magnetic fields and black hole rotation powers the jet acceleration
- Blandford-Znajek process, efficient if the rotational frequency of magnetic field is large wtr. to angular velocity of the black hole

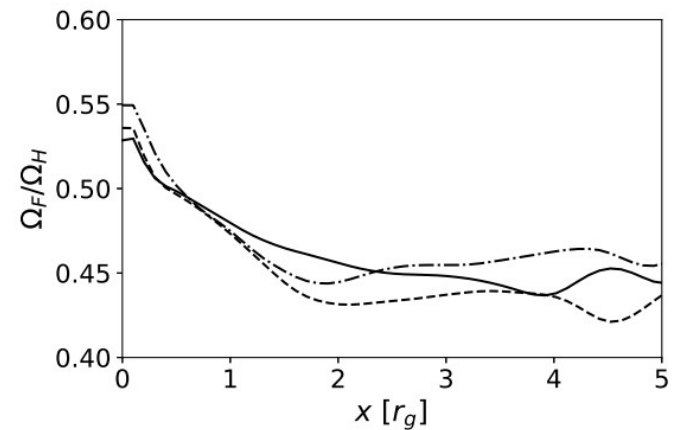
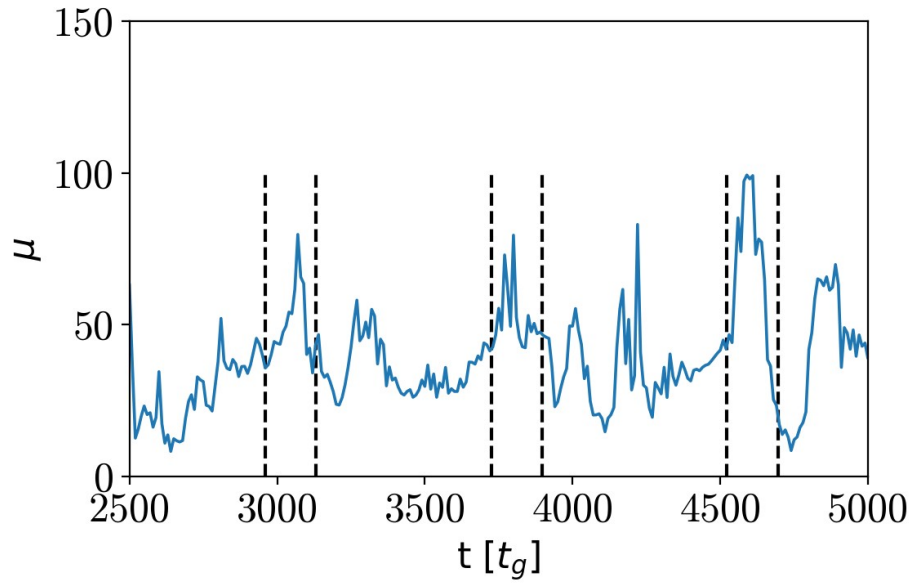
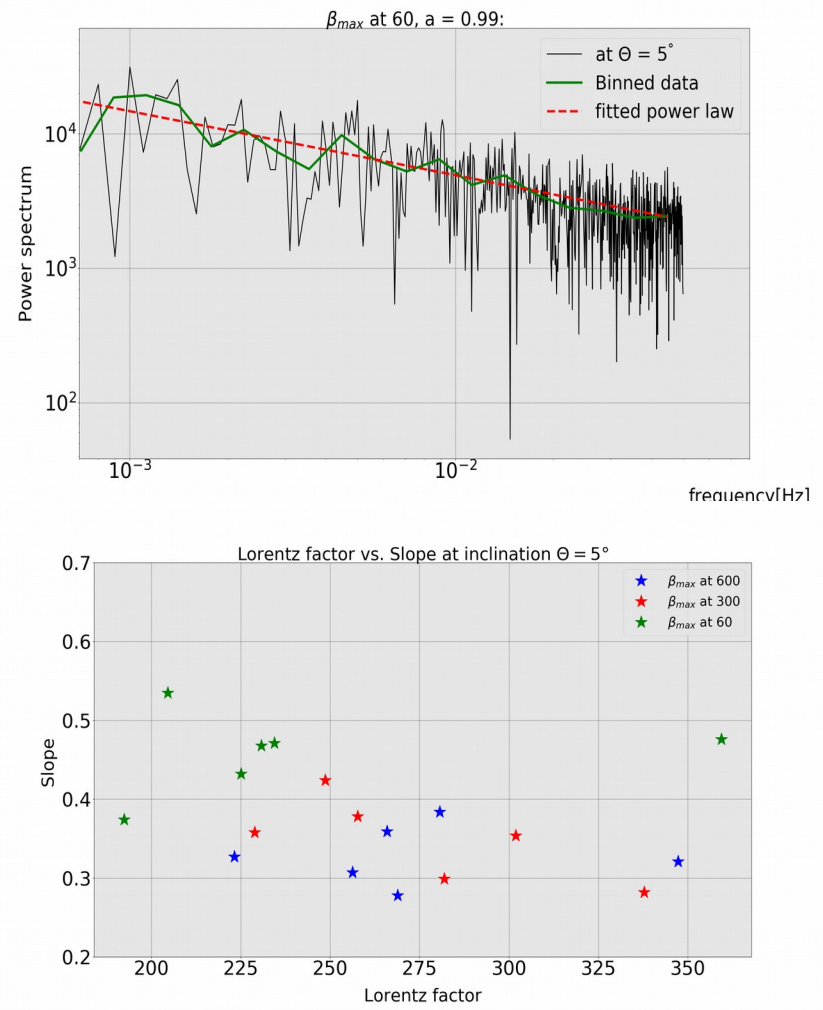


Fig from Sapountzis & Janiuk (2019, ApJ)

Variability of jets



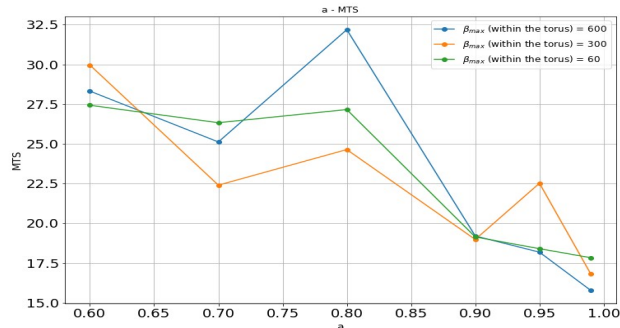
Time variability of jet energetics, as measured at specific point, at inner regions of jet .
 Variability is correlated with T_{MRI} , timescale of the fastest growing mode of magneto-rotational instability



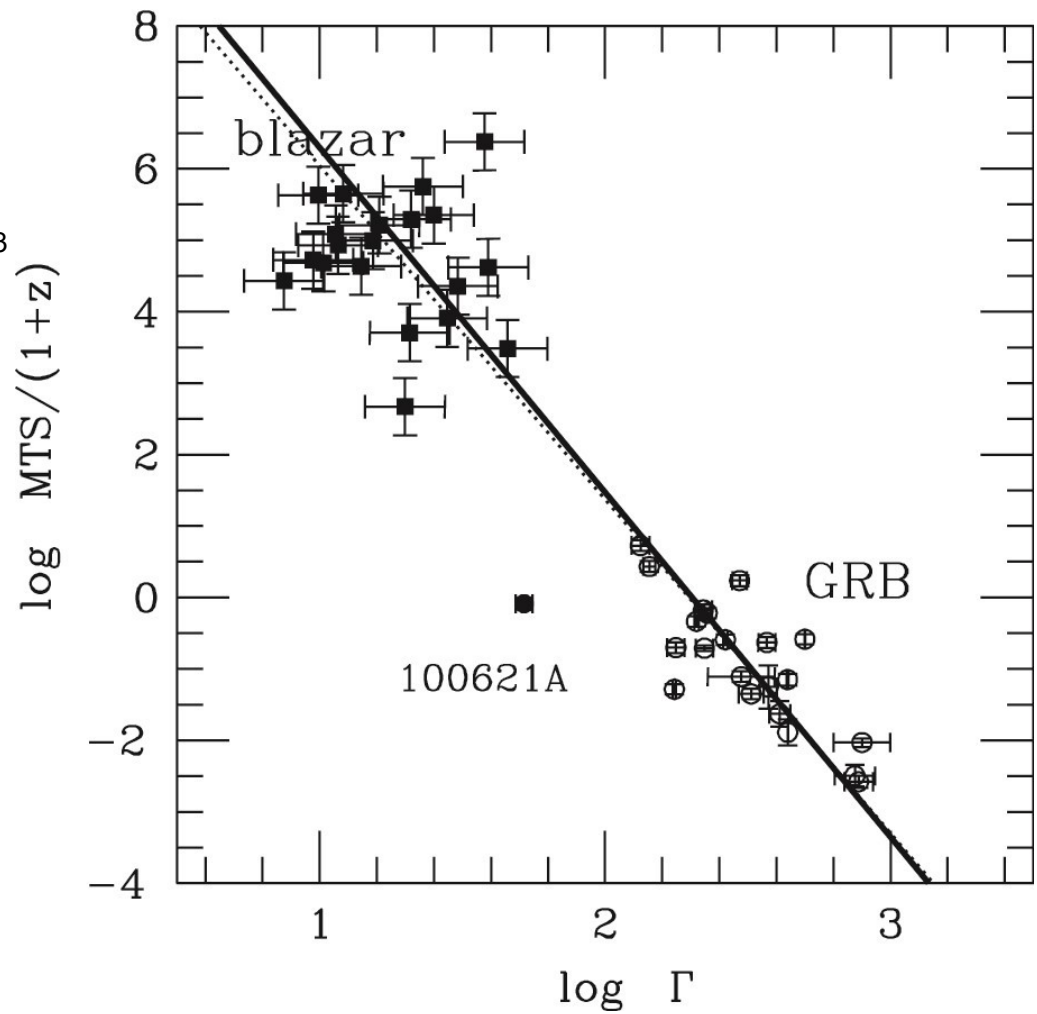
Power spectrum of model lightcurves. Power-law slope weakly depends on the black hole spin, while it seems to depend on jet Lorentz factor.

Variability correlations across mass scale

Correlations Γ - a and a -MTS are confirmed. Results scale with black hole mass: $MTS_s = MTS_{MBH} \times GM_{BH}/c^3$



See next talk by Bestin James



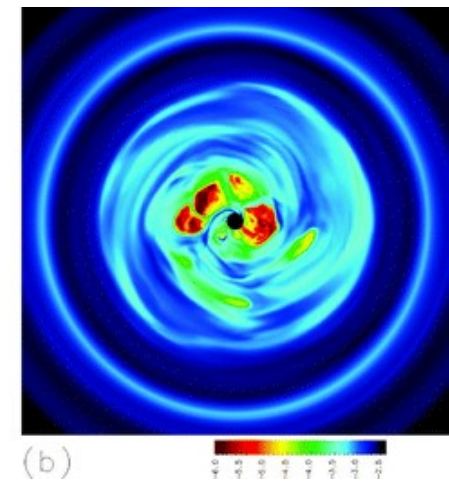
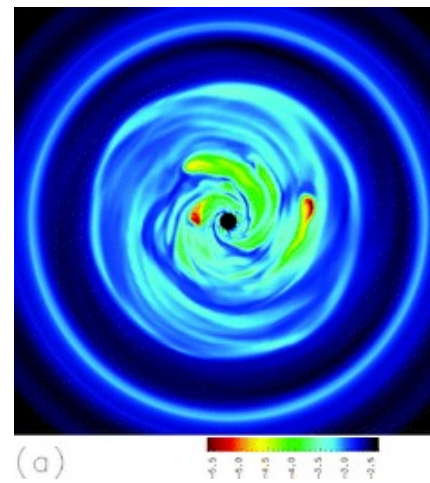
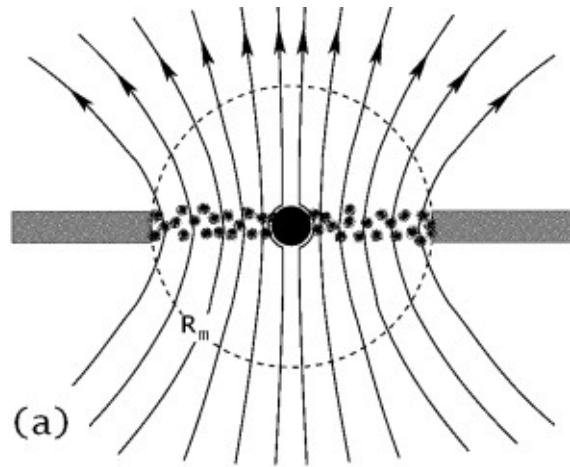
Joint correlation of $MTS \propto \Gamma^{-4.7 \pm 0.3}$ for blazar and GRB samples (Wu et al. 2016)

MAD mode of accretion

In the MAD mode, poloidal magnetic field is accumulating close to BH horizon, due to accretion

Field is prevented from escape as a result of inward pressure. It cannot fall into black hole either, while only the matter can fall in (Punsly 2001). The velocity of gas in this region is much smaller than free-fall.

- Axisymmetric case: inside magnetospheric radius, R_m , gas accretes as magnetically confined blobs (Narayan, Igumenschev, Abramowicz, 2003).

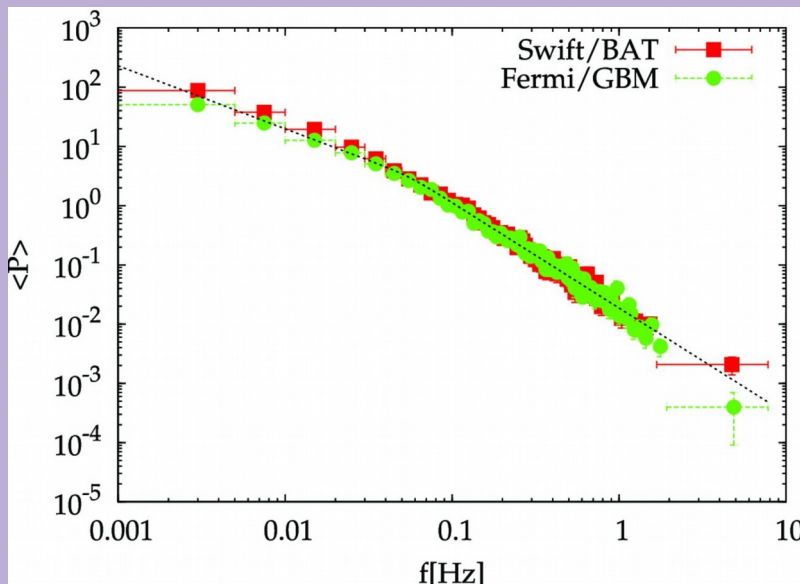


Non-axisymmetric case: gas forms streams which have to find the way towards back hole through magnetic reconnections and interchanges (e.g. Igumenshchev 2008)

Variable energy extraction from MAD disk

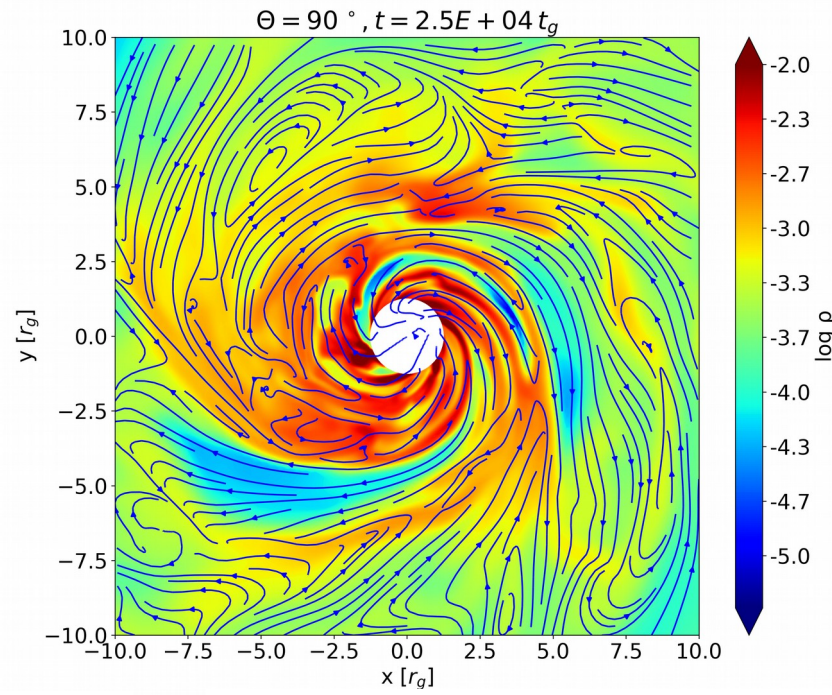
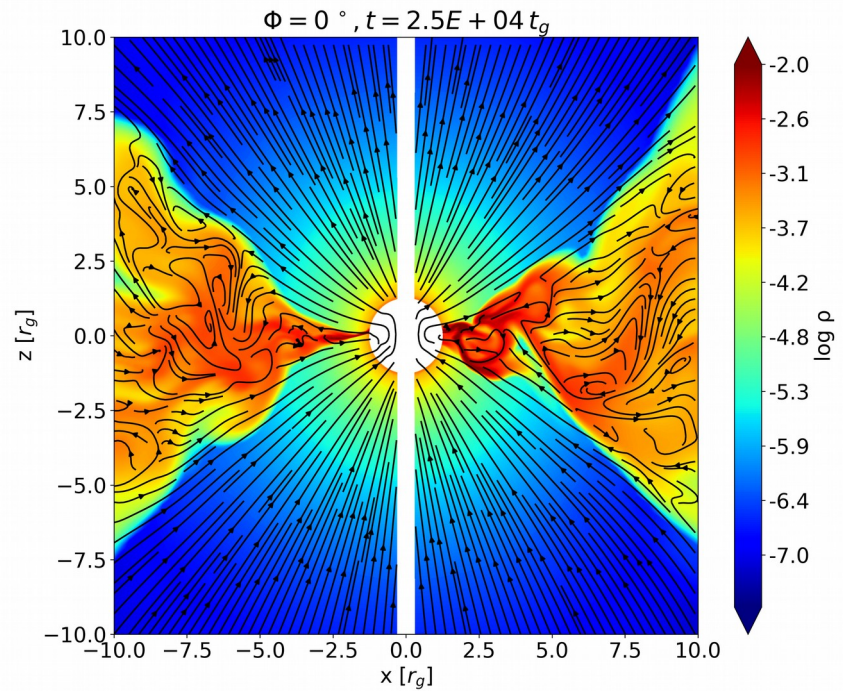
The ratio of total energy reaching infinity (radiative, mechanical, magnetic) to the rest mass energy in the MAD mode is large (cf. Bisnovatyi-Kogan & Ruzmaikin, 1974; 1976).

This large efficiency is obtained even for non-rotating black hole.
With a rotating black hole, one can extract in addition its rotational energy
(Tschekhovskoy et al. 2011).

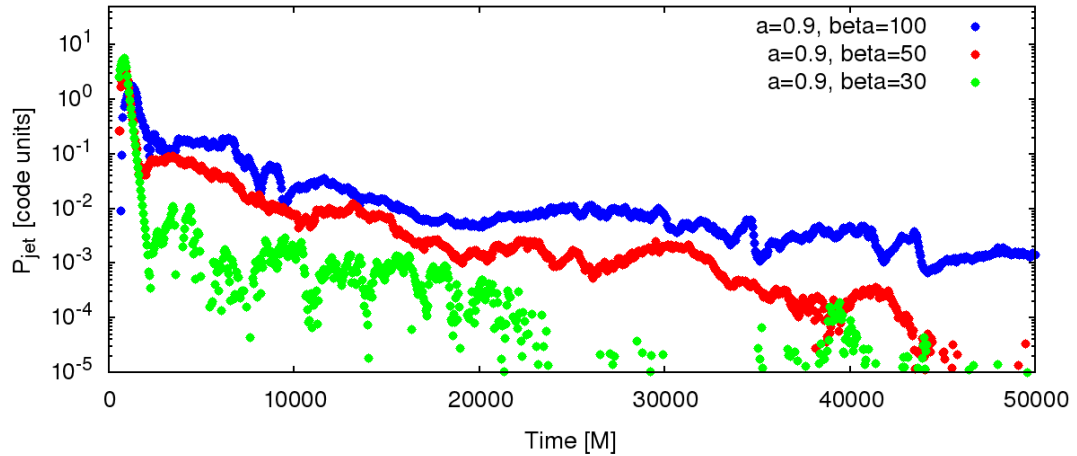


Models for the temporal variability of long gamma-ray bursts (GRBs) during the prompt phase (the highly variable first 100 s or so), were proposed in the context of a MAD around a black hole (see Lloyd-Ronning et al., 2016).

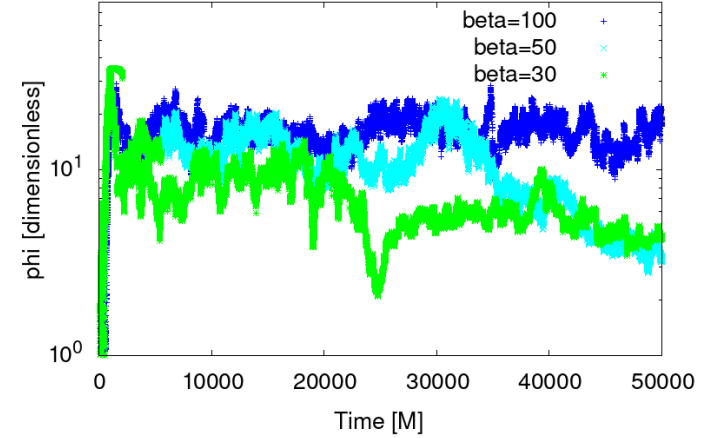
PDS spectra show power-law slopes between 1.49-1.65 (Dichiara et al. 2013)



Jet power, GRB models



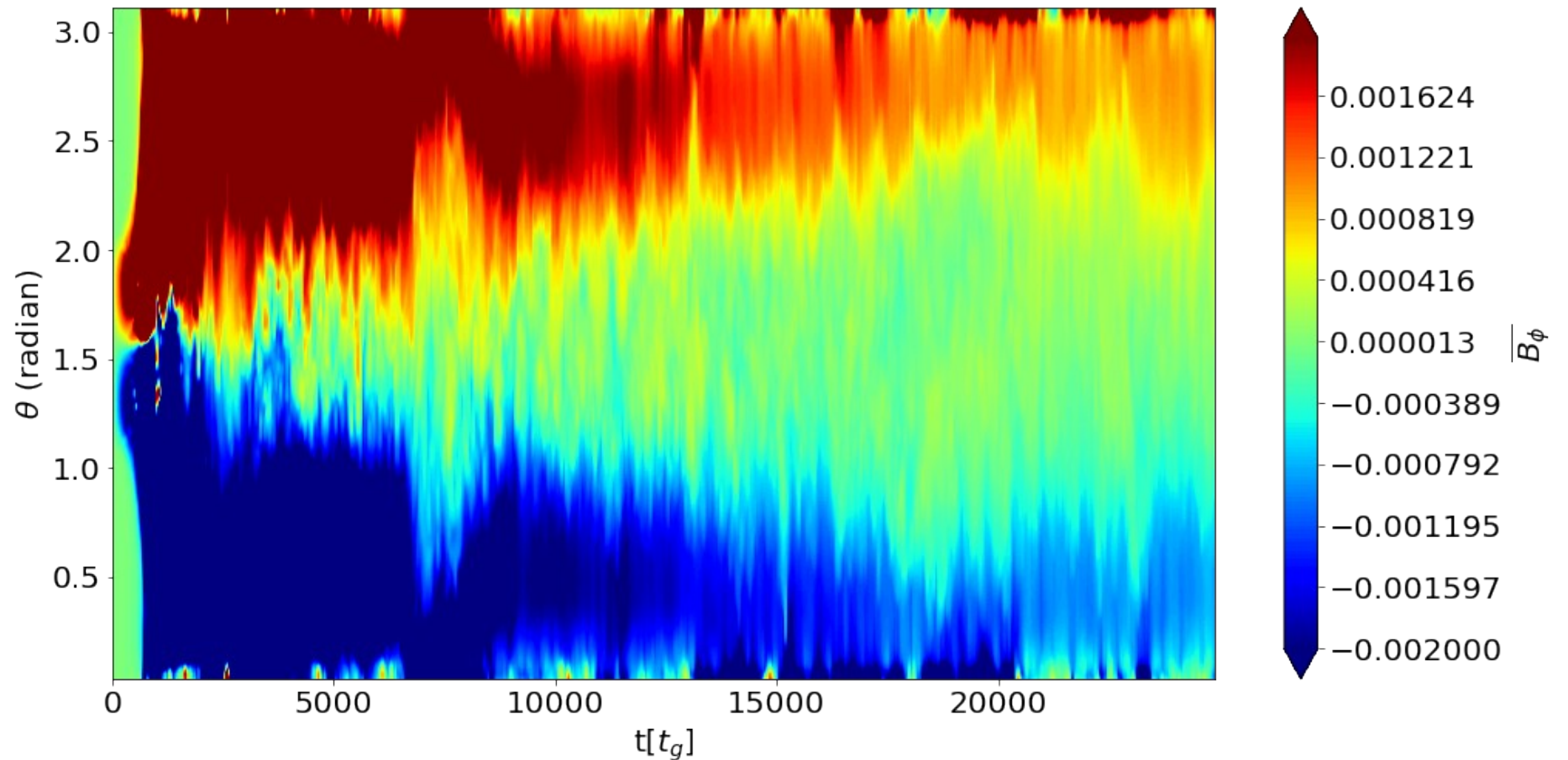
MAD parameter



A. Janiuk & B. James (2022, subm.);

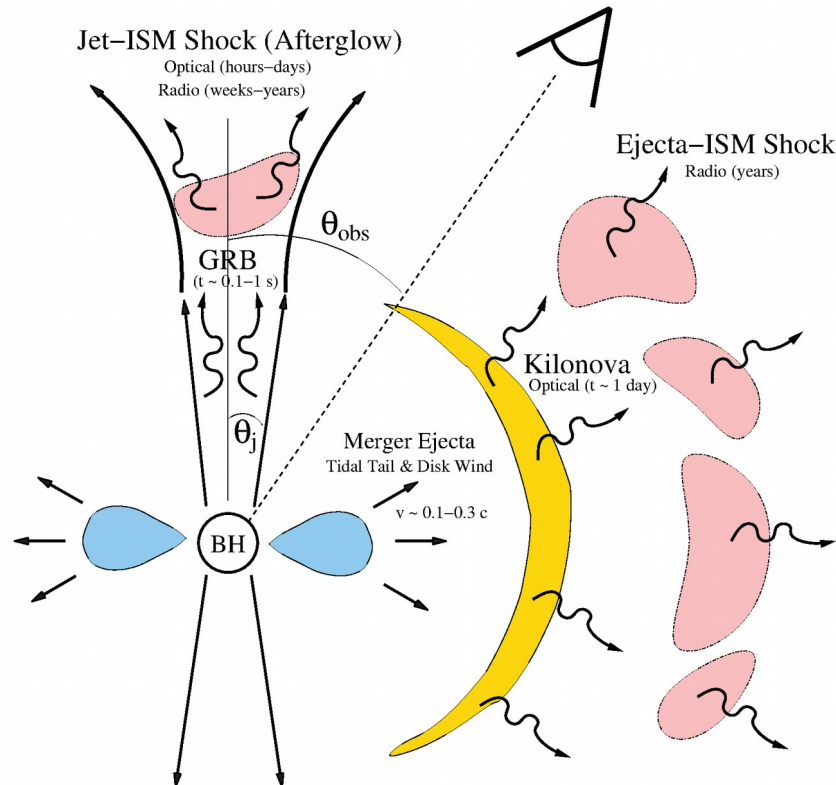
$$\varPhi_{\text{BH}} = \Phi_{\text{BH}} / 5 (r_g^2 c \dot{M})^{1/2}$$

Toroidal magnetic field evolution



see: B. James, A. Janiuk, F. Hossein-Nouri (2022).

Disk wind and jet: two types of outflow in GRBs



Potential electromagnetic counterparts of compact object binary mergers as a function of the observer viewing angle:

Accretion of a centrifugally supported disk (blue) powers a collimated relativistic jet, which produces a short GRB.

Kilonova is powered by postmerger ejecta, but the disk wind (equatorial outflows) also contributes to lower-energy signal.

Both jet and wind are powered by the Central Engine.

fig. B. Metzger (Living Reviews in Relativity, 2020).

Our GRMHD code with nuclear EOS

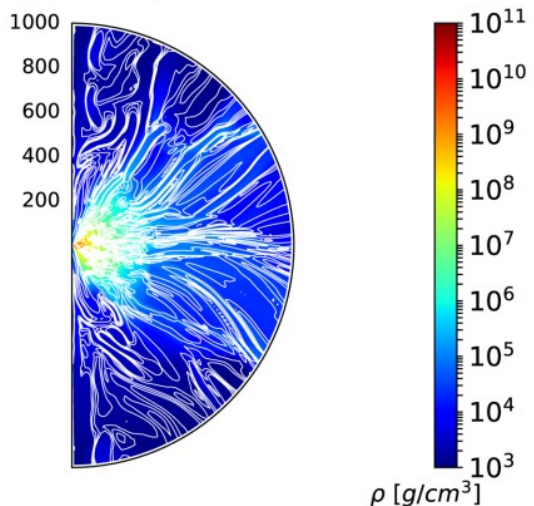
$$T_{(m)}^{\mu\nu} = \rho \xi u^\mu u^\nu + p g^{\mu\nu}$$

$$T_{(em)}^{\mu\nu} = b^\kappa b_\kappa u^\mu u^\nu + \frac{1}{2} b^\kappa b_\kappa g^{\mu\nu} - b^\mu b^\nu$$

$$T^{\mu\nu} = T_{(m)}^{\mu\nu} + T_{(em)}^{\mu\nu},$$

Original scheme:
2D, Gammie et al.(2003)

Density t=0.295

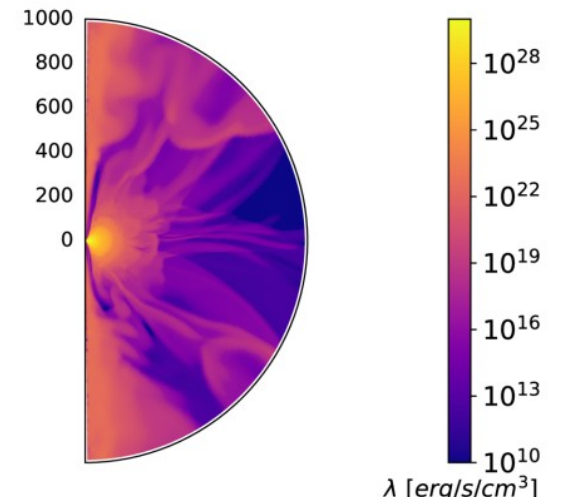


$$(\rho u_\mu)_{;\nu} = 0$$

$$T_{\nu;\mu}^\mu = 0.$$

- Hyperaccretion: rates of 0.01-10 M_s/s
- Plasma composed of free n, p, e+, e- pairs
- Chemical and pressure balance required by nuclear reactions: electron-positron capture on nucleons, and neutron decay (Reddy, Prakash & Lattimer 1998)
- Neutrino absorption & scattering, treated by grey-body approximation

Neutrino emissivity t=0.295



HARM_COOL code is suited for GRB: tabulated Equation of State of Fermi gas is computed numerically by solving the balance of beta reactions. Implemented into HARM scheme in Janiuk et al. (2013) and Janiuk (2017). cf. Fernandez et al. (2018)

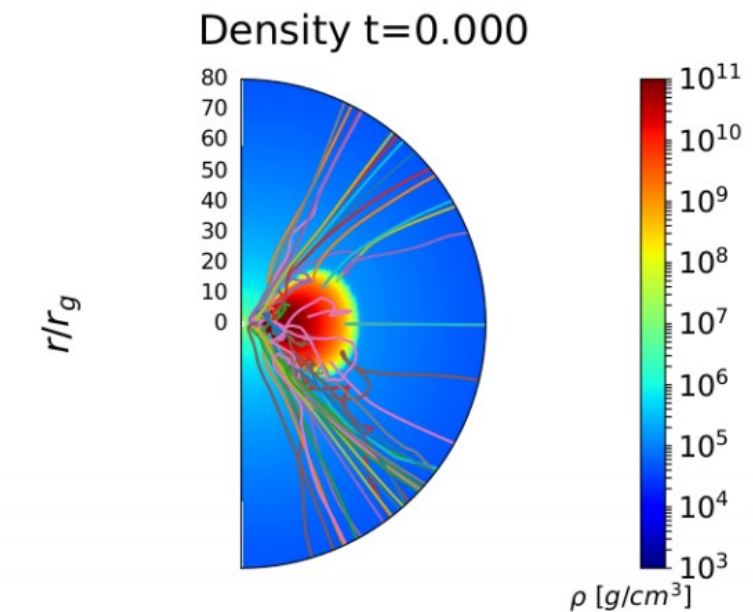
Outflow via disk wind

HARM-COOL (Janiuk, 2017, 2019).

- Fermi-gas EOS is implemented as tables, dynamically computed and filled with pressure, and entropy values as function of density and temperature
- Hybrid MPI-Open MP parallelisation; dumps in HDF5/Ascii format

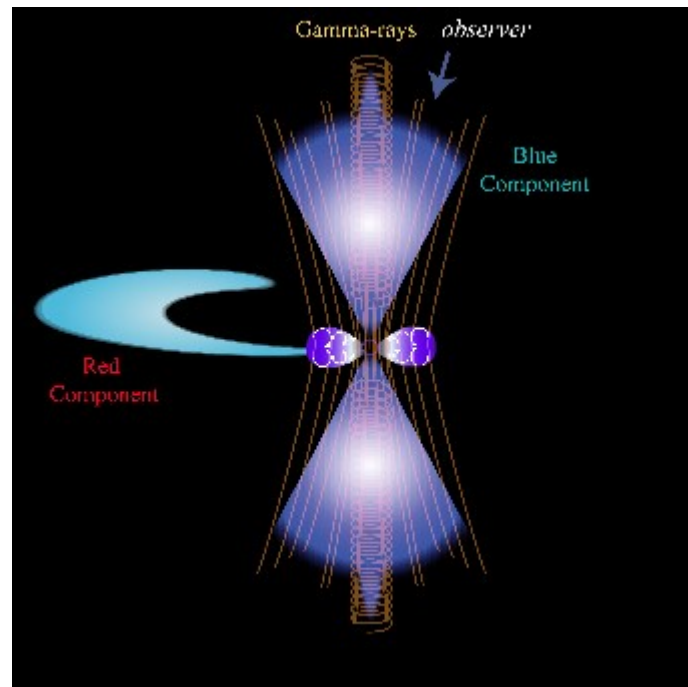
Code follows the wind outflow, and computes the trajectories, where mass is ejected in sub-relativistic particles.

Tracers distributed uniformly in rest-mass density inside initial torus (cf. Wu et al. 2016; Bovard & Rezzola 2017). Tracers store data about density, velocity, and electron fraction in the outflow.



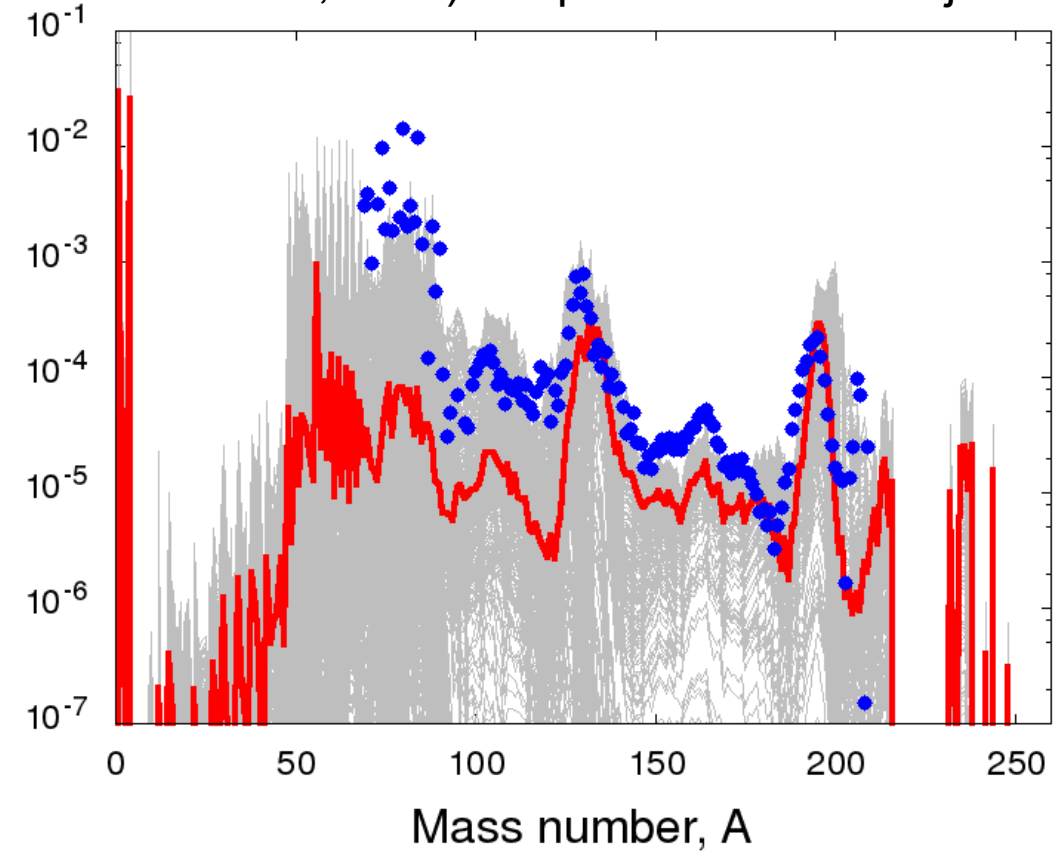
https://github.com/agnieszkajaniuk/HARM_COOL

Nucleosynthesis in disk wind



Schematic view of post-merger system and short GRB jet in GW 170817 (Murguia-Berthier et al., 2018)

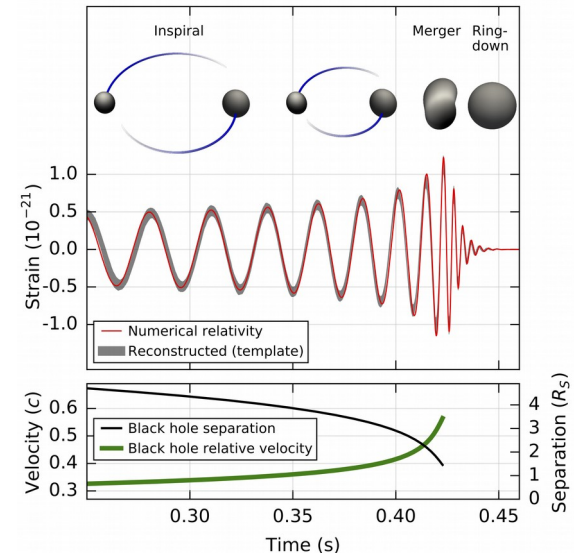
Heavy elements up to $A \sim 200$ (incl. Platinum, Gold) are produced in disk ejecta.



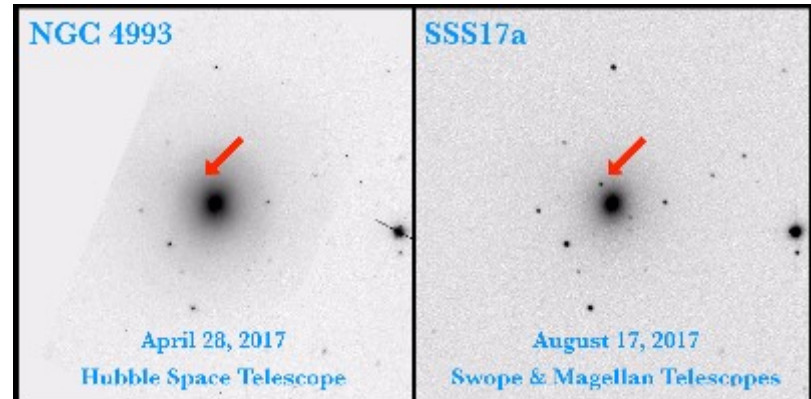
Results of simulation: nucleosynthesis in accretion disk wind (Janiuk, 2019, ApJ, 882, 163)

GW 170817

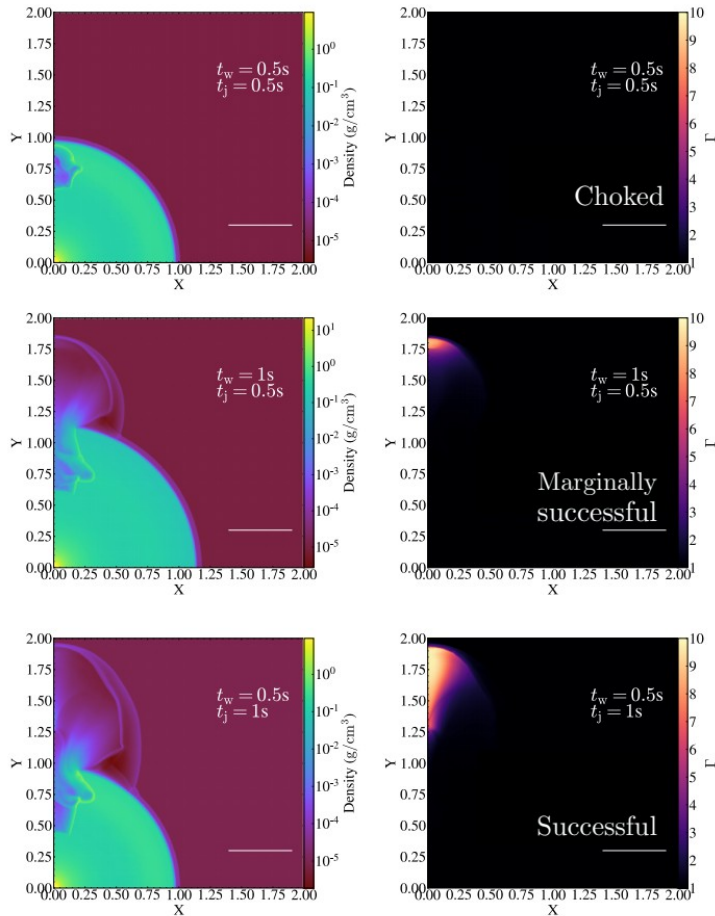
Double neutron stars formed a black hole after their merger.
During the inspiral phase,
gravitational waves were produced
After the merger, gamma-ray telescopes observed a **burst** of energy.
The time delay of 1.7 s may be associated with formation of HMNS



Rapidly fading electromagnetic transient in the galaxy NGC4993, was spatially coincident with GW170817 and a weak short gamma-ray burst (e.g., Smartt et al. 2017; Zhang et al. 2017, Coulter et al. 2017)

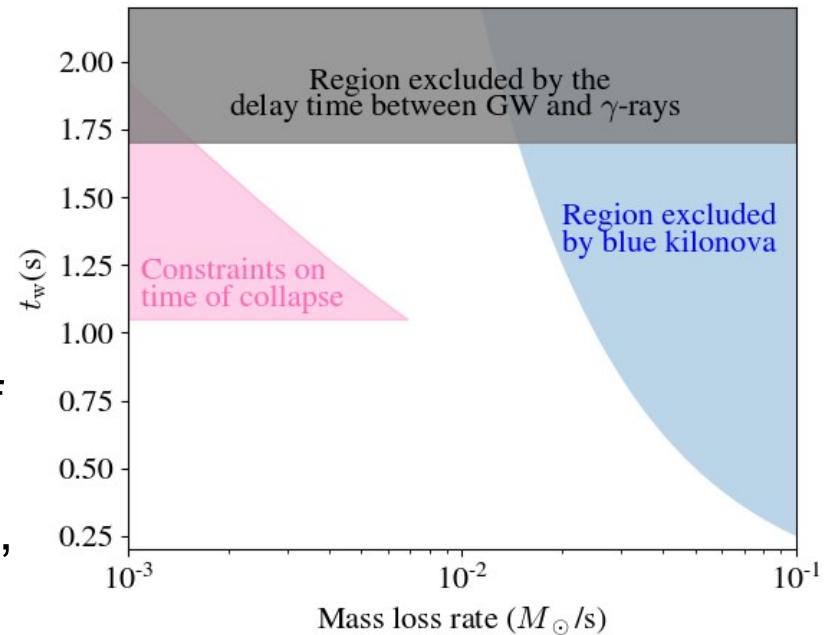


Chocked jet in GW 170817



Constraints for wind time t_w as a function of mass loss. **GW 170817:** jet energy of $5 \times 10^{48}\text{-}10^{50}$ erg, initial opening angle: 9-20°, Lorentz factor $\Gamma=100\text{-}1000$

- Expansion of the jet is affected by the properties of the wind through which it propagates
- Various models of accretion disk wind: neutrino-driven, magnetically driven

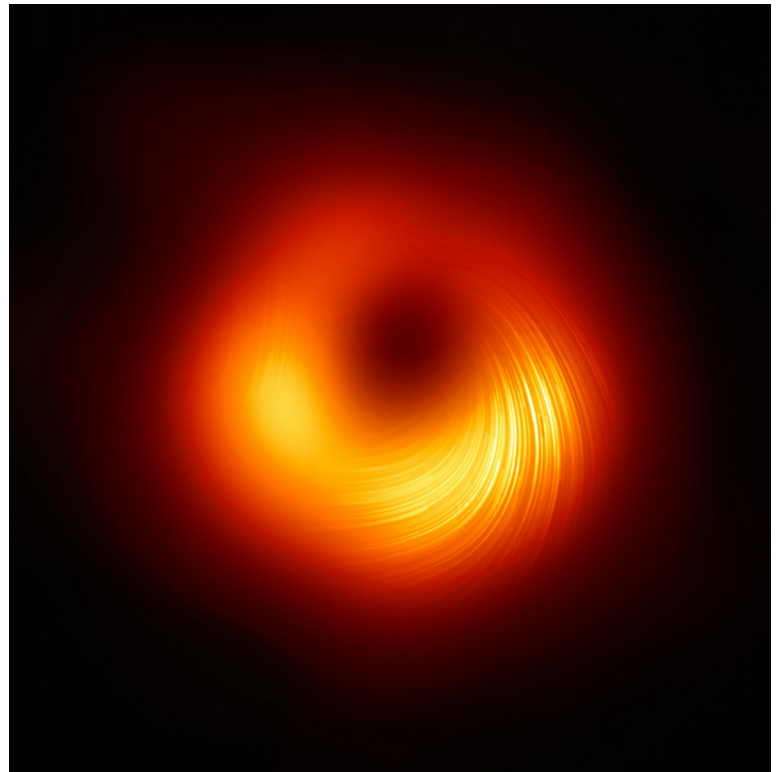


(A. Murguia-Berthier, E. Ramirez-Ruiz, AJ, S. Rosswog, et al., 2021, ApJ)

Black Hole horizon

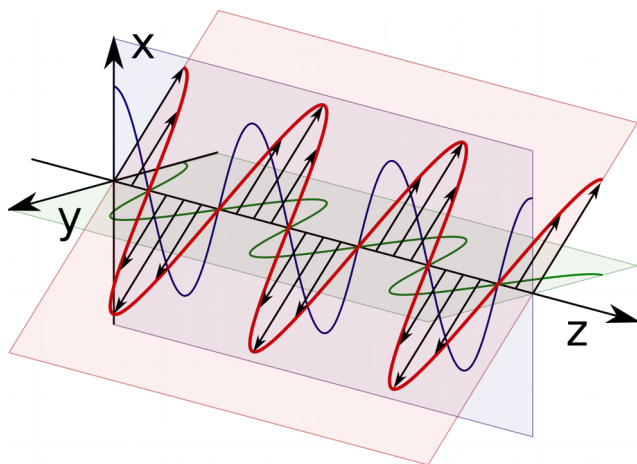
The EHT collaboration produced first ever image of a supermassive black hole in M87

Polarisation measurements are signature of magnetic fields close to the horizon of black holes



Polarized radiation transport

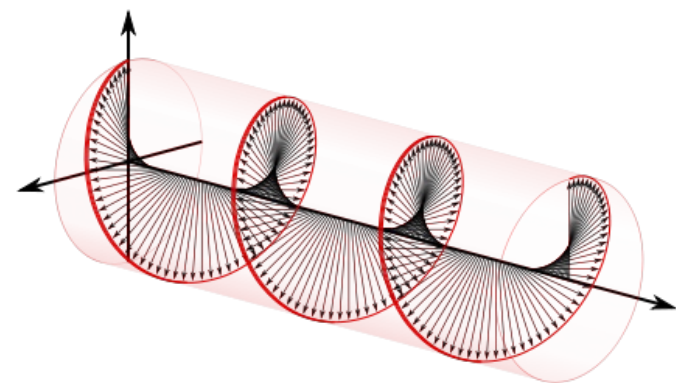
Linear polarisation: electromagnetic field is confined to the plane along the direction of the wave (light) propagation



Fractional polarisation is described by the Stokes vector, $S=(I, Q, U, V)$.

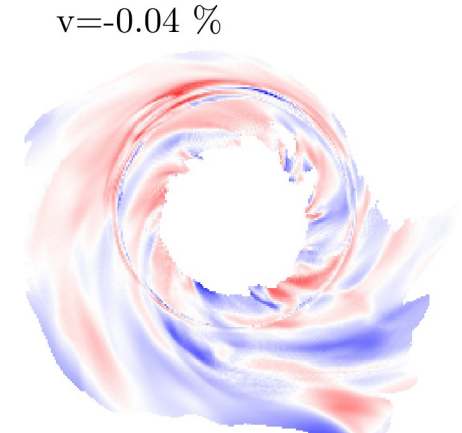
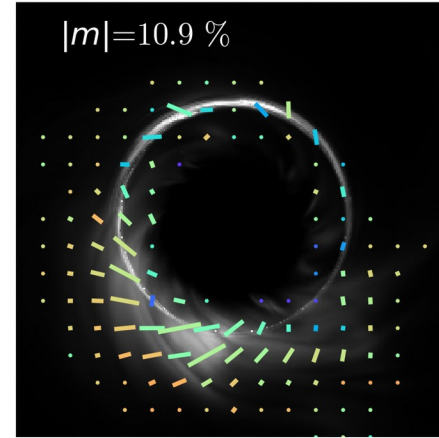
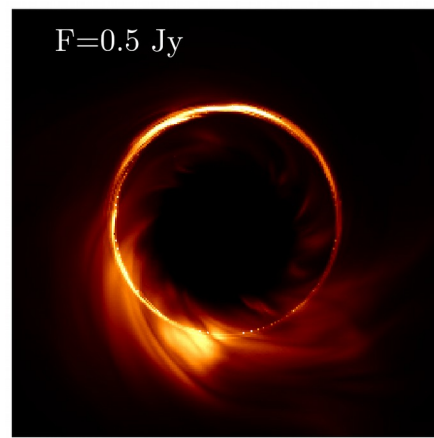
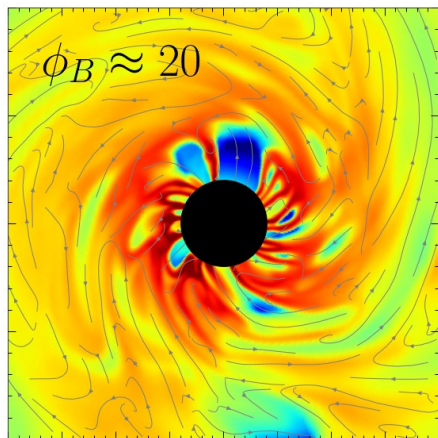
Faraday effect : Faraday conversion means that polarisation rotation is proportional to the projection of the magnetic field on the direction of light propagation

Circular polarisation: electromagnetic field rotates at constant rate in a plane perpendicular to the direction of the EM wave propagation



We use **iPole: ray-tracing code** for polarized radiative transport, under two representations. In coordinate frame, the code transports the coherency tensor. In plasma frame, it evolves the Stokes parameters, under emission, absorption, and Faraday conversion (**Mościbrodzka & Gammie, 2018**)

Polarisation of MAD disk close to horizon



Polarimetric images of MAD disk, at equatorial plane. Parameters: $a=0$, $\beta=30$, and ion-to-electron temperature ratio $R_h = 1$. Viewing angle $i=160$ deg.

Details in Mościbrodzka, Janiuk & De Laurentis (2021, MNRAS)

Summary

- Jets from MAD disks are highly variable, both in GRB and AGN scenarios. Broad-band correlations between jets Lorentz factors and variability timescales from blazars to GRBs are reproduced by numerical simulations.
- MHD simulations show that rotational instabilities have imprint on the variability of the jet. The same MHD mechanism drives the disk-wind.
- The r – process nucleosynthesis in the magnetically driven accretion disk outflows can provide additional contribution to the kilonova emission, apart from the BNS merger ejecta
- Jet interactions with wind shape its radiative properties and together with pre-merger dynamical ejecta may explain time-delay between GW and GRB signals. Wind can be responsible for jet quenching in GRBs.
- There is no clear analogy of jet-wind interaction in AGN case.
- Polarisation measurements of near horizon region, incl. Strength of Faraday conversion, should validate the case of MAD scenario in AGN.



NARODOWE CENTRUM NAUKI